Near field imaging of terahertz focusing onto rectangular apertures

M. A. Seo,[1] A. J. L. Adam,[2] J. H. Kang,[3] J. W. Lee,[1] K. J. Ahn,[1] Q. H. Park,[3] P. C. M. Planken,[2†*] and D. S. Kim[1‡*]

[1]*Department of Physics and Astronomy, Seoul National University, Seoul 151-747, Korea*
[2]*Faculty of Applied Sciences, Delft University of Technology, Lorentzweg 1, 2628 CJ Delft, The Netherlands*
[3]*Department of Physics, Korea University, Seoul 136-701, Korea*
[*]*Corresponding author: ‡dsk@phya.snu.ac.kr and †P.C.M.Planken@tudelft.nl.*

Abstract: We performed terahertz near-field experiments on single rectangular holes with various lengths grown on an electro-optic crystal substrate with $\lambda/100$ resolution. We find that the near-field amplitude becomes proportionally larger as the rectangle becomes narrower, strongly suggesting that a constant energy passes through even for a very narrow slit. The occurrence of a large field enhancement at the fundamental localized resonance is discussed confirming the funneling of energy at the near-field.

OCIS codes: (180.0180) Microscopy; (260.3090) Far-infrared; (320.7150) Ultrafast spectroscopy.

References and links

1. J. H. Poynting, "On the Transfer of Energy in the Electriomagnetic Field," Philosophical Trans. of the Royal Soc. London **175**, 343-361 (1884).
2. E. Abbe, "Beitrage zur Theorie des Mikroskops und der Mikroskopischen Wahrnehmung," Arch. Mikrosk. Anat. **9**, 413-468 (1873).
3. Y.-M. Shin, J.-K. So, K.-H. Jang, J.-H. Won, A. Srivastava, and G.-S. Park, "Evanescent Tunneling of an Effective Surface Plasmon Excited by Convection Electrons," Phys. Rev. Lett. **99**, 147402, (2007).
4. J. W. Lee, M. A. Seo, D. J. Park, D. S. Kim, S. C. Jeoung, Ch. Lienau, Q-Han. Park, P. C. M. Planken, "Shape resonance omni-directional terahertz filters with near-unity transmittance," Opt. Express **14**, 1253-1259 (2006).
5. F. Miyamaru, M. Tanaka, and M. Hangyo, "Effect of hole diameter on terahertz surface-wave excitation in metal-hole arrays," Phys. Rev. B **74**, 153416 (2006).
6. J. W. Lee, M. A. Seo, D. H. Kang, K. S. Khim, S. C. Jeoung, and D. S. Kim, "Terahertz Electromagnetic Wave Transmission through Random Arrays of Single Rectangular Holes and Slits in Thin Metallic Sheets," Phys. Rev. Lett. **99**, 137401 (2007).
7. M. Golosovsky and D. Davidov, "Novel millimeter-wave near-field resistivity microscope," Appl. Phys. Lett. **68**, 1579-1581 (1996).
8. T. W. Ebbesen, H. J. Lezec, H. F. Ghaemi, T. Thio, and P. A. Wolff, "Extraordinary optical transmission through sub-wavelength hole arrays," Nature **391**, 667-669 (1998).
9. B. S. Williams, "Terahertz quantum-cascade lasers," Nat Photon **1**, 517-525 (2007).
10. W. C. Hurlbut, Yun-Shik Lee, K. L. Vodopyanov, P. S. Kuo, and M. M. Fejer, "Multiphoton absorption and nonlinear refraction of GaAs in the mid-infrared," Opt. Lett. **32**, 668-670 (2007).
11. J. B. Masson, M. P. Sauviat, J. L. Martin, and G. Gallot, "Ionic contrast terahertz near-field imaging of axonal water fluxes," Proc. Nat. Acad. Sci. USA **103**, 4808-4812 (2006).
12. M. A. Seo, A. J. L. Adam, J. H. Kang, J. W. Lee, S. C. Jeoung, Q. H. Park, P. C. M. Planken, and D. S. Kim, "Fourier-transform terahertz near-field imaging of one-dimensional slit arrays: mapping of electric-field-, magnetic-field-, and Poynting vectors," Opt. Express **15**, 11781-11789 (2007).
13. A. J. L. Adam, J. M. Brok, M. A. Seo, K. J. Ahn, D. S. Kim, J. H. Kang, Q. H. Park, M. Nagel, amd P. C. M. Planken, "Advanced terahertz electric near-field measurements at sub-wavelength diameter metallic apertures," Opt. Express **16**, 7407-7417 (2008).
14. N. C. J. Van der Valk, T. Wenckebach, and P. C. M. Planken, "Full mathematical description of electro-optic detection in optically isotropic crystals," J.Opt. Soc. Am. B **21**, 622-631 (2004).
15. D. F. Nelson and E. H. Turner, "Electro-optic and piezoelectric coefficients and refractive index of gallium phosphide." J. Appl. Phys. **39**, 3337-3343 (1968).
16. A. J. Huber, F. Keilmann, J. Wittborn, J. Aizpurua, and R. Hillenbrand, "Terahertz Near-Field Nanoscopy of Mobile Carriers in Single Semiconductor Nanodevices," Nano Lett. **8**, 3766 (2008).

#102270 - $15.00 USD Received 1 Oct 2008; revised 19 Nov 2008; accepted 20 Nov 2008; published 25 Nov 2008

17. N. C. J. van der Valk and P. C. M. Planken, "Electro-optic detection of sub-wavelength terahertz spotsizes in the near-field of a metal tip," Appl. Phys. Lett. **81**, 1558-1560 (2002).
18. F. Buersgens, R. Kersting, and H. –T Chen, "Terahertz microscopy of charge carriers in semiconductors," Appl. Phys. Lett. 88, 112115 (2006).
19. F. J. Garcia-Vidal, E. Moreno, J. A. Porto, and L. Martin-Moreno, "Transmission of light through a single rectangular hole," Phys. Rev. Lett. **95**, 103901 (2005).
20. D. M. Pozar, "Reciprocity method of analysis for printed slot-coupled microstrip antennas," IEEE Trans. Antennas Propag. **34**, 1439-1446 (1986).
21. H. A. Bethe, "Theory of Diffraction by Small Holes," Phys. Rev. **66**, 163-182 (1944).
22. C. J. Bouwkamp, "On the diffraction of electromagnetic waves by small circular disks and holes," Philips Res. Rep. **5**, 401-422 (1950).
23. M. Born and E. Wolf, *Principles of Optics* (Pergamon Press, Oxford, 1964).

Poynting's law [1], which governs electromagnetic energy flow in space around conductors, is equivalent in its form to the continuity equation in fluid dynamics. Since continuity equations naturally allow funneling through a small opening, we may anticipate that a large amount of electromagnetic energy can in principle concentrate and flow through a small aperture in perfect conductor. For this electromagnetic funneling to occur, energy conservation demands large field enhancement at the aperture. In this sense, a well-designed aperture can be the most efficient way of focusing electromagnetic energy beyond diffraction limit [2], provided that a resonant condition for large near-field enhancement is met. This type of near-field focusing is implicit in many experiments, including far-field transparency [3, 4] at the fundamental resonance [5-7]. Near-field enhancement [8] and focusing would be particularly desirable in the terahertz range where most tabletop laboratory sources are too weak to induce, for example, nonlinear effects or to detect single molecules [9-11].

Here, we show extreme near-field measurements of rectangular apertures in the THz frequency range, using terahertz time-domain spectroscopy (THz-TDS) [12, 13]. This technique allows us to measure the near-field profile of an electric-field component at each frequency in the broad spectral range of 0.1 to 1.5 THz. The Fourier-transform near-field microscopic technique is used to obtain time and frequency domain near-field images of the tangential electric field transmitted through the single rectangular apertures. Our sample consists of rectangular holes made in a metallic sheet deposited on a (110) oriented GaP crystal, which acts both as a dielectric support and as the field-detecting electro-optic crystal. In this orientation of the crystal, with the probing light polarization along the *x*-axis, we detect the horizontal component of the terahertz electric field along the *x*-axis [14, 15] while the long axis of the rectangle is along the y-direction (Fig. 1). Our system has a spatial resolution of less than 10 μm and the direct deposition of metal onto the electro-optic crystal allows near-field detection with extreme subwavelength resolution in the THz frequency range. Recently, higher spatial resolution of up to 40 *nm* [16] has been realized with an antenna-scattering technique [17, 18] although these methods are not capable of separately measuring the three vector components of the electric field. The most interesting aspect of our results is that the resonantly enhanced near-field amplitude becomes larger as the slit narrows. This is consistent with the constant energy funneling through the narrow slit at the fundamental shape resonance.

We measure the *x*-component electric field around a rectangle of a_x =10 μm and a_y =300 μm with a scan area of 200 μm x 400 μm. At each pixel, time-domain THz signal is acquired. Fast Fourier Transforming (FFT) the time traces at each position results in the frequency-domain images, complete with amplitude and phase [12]:

$$E_x(x, y, \omega) = \frac{1}{2\pi}\int E_x(x, y, t)e^{i\omega t}dt \qquad (1)$$

#102270 - $15.00 USD Received 1 Oct 2008; revised 19 Nov 2008; accepted 20 Nov 2008; published 25 Nov 2008

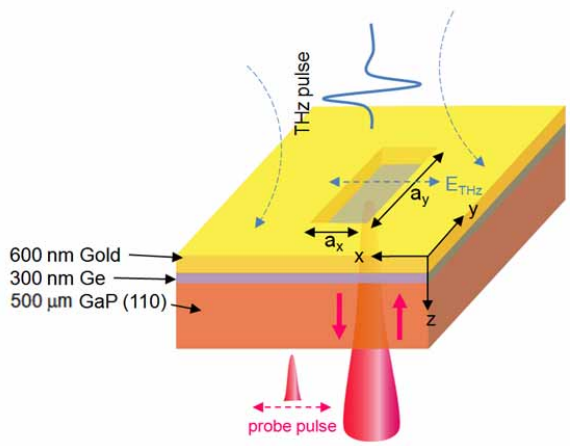

Fig. 1. Tehahertz near-field measurement of a single rectangular hole of sides a_x and a_y perforated in a gold metal film deposited on a piece of electro-optic crystal GaP. This system is normally irradiated by an *x*-polarized terahertz plane wave and electro-optic sampling is performed using a terahertz time domain spectroscopy.

The experimental image reconstruction based on Eq. (1), with proper normalization against the incoming terahertz spectrum, allows steady-state images at each frequency component. Figures 2(a), (b), (c), and (d) show the field amplitude images at 0.1 THz, 0.2 THz, 0.6 THz, and 1.0 THz, respectively. The brightest image occurs at around 0.2 THz, which is close to the predicted fundamental localized surface plasmon resonance on the crystal side: the resonance frequency is $\sim c/(2na_y)$ where n is the index of refraction of the electro-optic crystal, instead of $c/(2a_y)$ appropriate for the free standing case. Weak but noticeable higher order modes contribution can be seen at higher frequencies: 0.6 THz (Fig. 2(c)) and at 1.0 THz (Fig. 2(d)). These results show that our Fourier-transform imaging technique captures deep near-field. We now compare different slit widths while keeping the slit length constant.

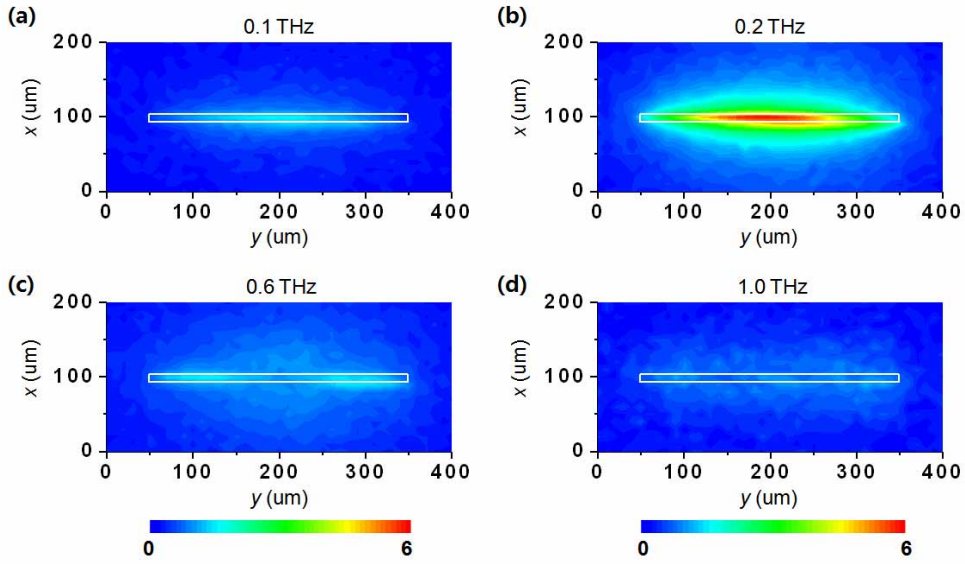

Fig. 2. Fourier-transformed images of E_x component at a rectangle of 10 μm width and 300 μm length. The E_x images are shown at (a), 0.1 THz, (b), the resonance frequency, 0.2 THz, (c), 0.6 THz, and (d), 1.0 THz, respectively.

#102270 - $15.00 USD Received 1 Oct 2008; revised 19 Nov 2008; accepted 20 Nov 2008; published 25 Nov 2008

Shown in Fig. 3(a), 3(b), and 3(c) are the images for samples with a_x=100, 50 μm, and 10 μm, respectively for a fixed length of a_y=300 μm at 0.2 THz, which is the approximate resonant frequency for all three samples. A cut through the width of the rectangle is shown on the right side of each image. For both Fig. 3(a) and 3(b), the signal abruptly turns into a plateau within a single pixel at the edge of the slit. This demonstrates that the spatial resolution of the images is better than the 10 micron step size. For each sample, the near-field amplitudes at the high-frequency plateau in the frequency range of 0.7-1.2 THz, taken at the center pixel (Fig. 3(d)), are assumed equal. Since we expect that the near-field amplitude far above the cut-off would approximately be equal to that of the incident wave regardless of the slit width [6, 19, 20], this scaling allows us to compare different samples and also to estimate the actual near-field enhancement relative to the incident field.

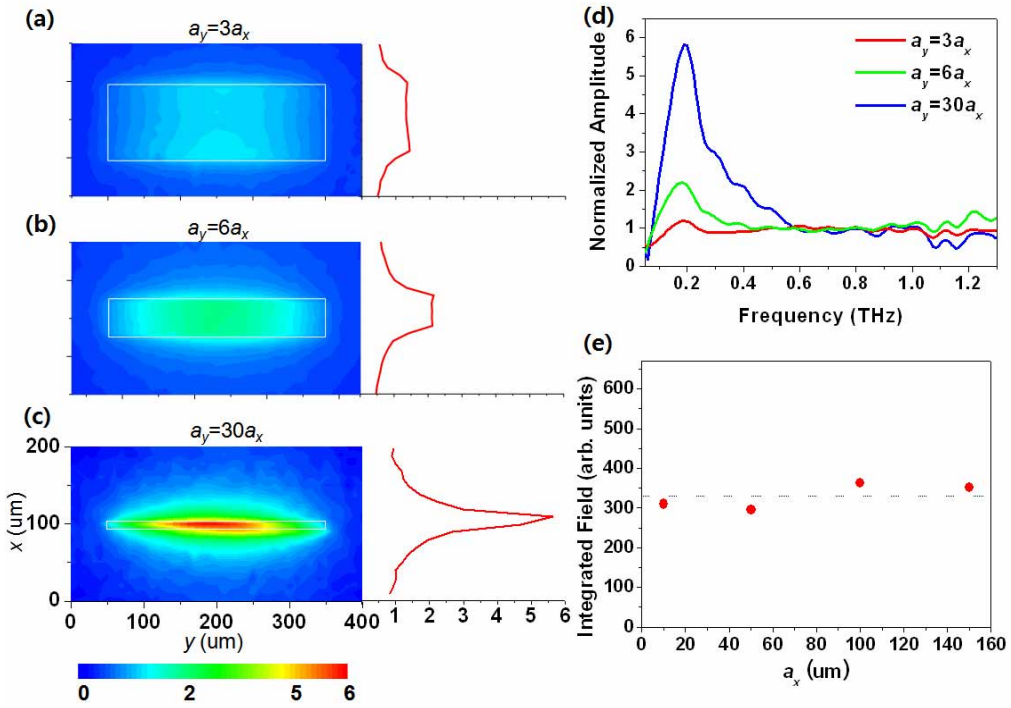

Fig. 3. Fourier-transformed images of E_x component around single rectangles of different widths for a fixed length. The images are shown for (a), a_x =100 μm, (b), a_x=50 μm, and (c), a_x=10 μm, respectively. The length is fixed at 300 μm. The red line on the right side is cut through the center of the rectangle. The spectra at the center of the slits for various slit aspect ratios are shown. These spectra are normalized against the high frequency plateaus (d). The integrated field amplitude over the area of the rectangle versus the width of the rectangle is shown (e). The dotted line denotes the average of the integrated values.

In Fig. 3(a), 3(b), and 3(c), with narrowing slit widths, the scaled near-field amplitude at resonance keeps increasing. At the narrowest slit shown in Fig. 3c, the near-field enhancement reaches six and the full-width-at-half maximum of the sharp peak is 1-2 pixels only. It is interesting to note that the area-integrated field amplitude remains nearly constant (Fig. 3(e)) for four different slit widths investigated. In the following, we discuss the implication of the constancy of the integrated field amplitude.

We expect that the horizontal magnetic field remains nearly constant around a sub-wavelength aperture punctured in a perfectly conducting sheet of metal [21, 22]. Then, the constancy of the area integrated electric field implies that a constant power flows through the slit at resonance, accompanied by a field enhancement inversely proportional to the width. A

#102270 - $15.00 USD Received 1 Oct 2008; revised 19 Nov 2008; accepted 20 Nov 2008; published 25 Nov 2008

recent calculation predicts this funneling of constant power through the slit regardless of its width [19]: for rectangles with an extreme aspect ratio of $a_x << a_y$, the area-normalized transmittance at resonance increases with the decreasing slit width as $T_{res} \approx (3/\pi)a_y / a_x \sim a_y / a_x$.

The physics of this seemingly counter-intuitive result of constant power flow can be best understood if we consider the complementary image of the slit, which is a narrow, half-wavelength antenna. We expect that the power absorbed by a half-wavelength center-fed rectangular antenna operating at its fundamental resonance, with the incoming polarization along the antenna-axis, would not sensitively depend on the width of the antenna, as long as the perfect conductor approximation is valid. Using the vector Babinet's principle arguments [23], we anticipate that the power transmitted through a rectangular slit would essentially be constant when the incoming polarization is perpendicular to the long-axis, regardless of the slit-width. The constancy of the area-integrated electric field and Poynting vector is also confirmed by finite-difference-time-domain (FDTD) calculations using the same sample parameters as in the experiments.

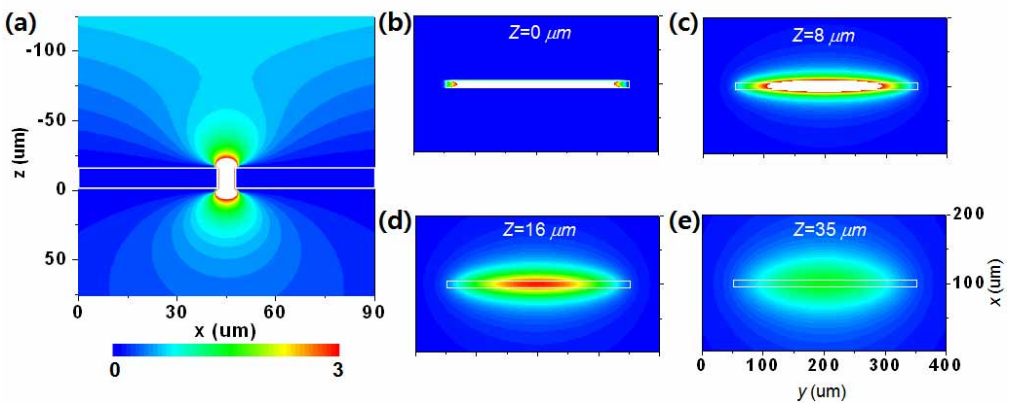

Fig. 4. FDTD simulated images. A side view of an FDTD simulated image describing energy focusing onto the single slit of 10 μm width and 300 μm length at the fundamental resonance of 0.2 THz (a). FDTD simulations for the same slit at z = 0 μm (b), z=8 μm (c), z=16 μm (d), and z=35 μm (e), respectively.

Finally, we discuss why we probe such deep near-field as is evident from the image quality. Figure 4(a) shows a cross-sectional view of the electric field amplitude using a finite-difference-time-domain (FDTD) simulation at the resonance frequency 0.2 THz for the a_y/a_x=30 case. The top part is for the air side and the bottom for the crystal side. The funneling process is clearly visible in this simulation. In experiments, the crystal detects a form of an integrated signal by the electro-optic sampling process at the exit side. What then is the effective distance away from the surface that we are probing? If we were to be probing precisely at the metal-crystal interface z=0, the tangential electric field should vanish and the images would reproduce the slit-shape, with the largest resonant field amplitude possible as shown in Fig. 4(b) (about 15 relative to the incident wave of amplitude 1, at the center). As we increase the distance away from the slit, the image blurs and the amplitudes decrease as shown in Fig. 4(c), 4(d), and 4(e). Based on the remarkable similarity between the simulated image at z=16 μm and the experimental image of Fig. 3(c), we estimate that our experiments probe an *effective z* of about 16 μm, in the same range as the slit width and about one hundredth of the vacuum wavelength at resonance. Considering that our electro-optic sampling signal is integrated over the entire crystal thickness of 500 μm, such small *effective z* warrants our attention. We believe that the answer to this *near-sightedness* of our experiment can be found in Fig. 4(a): the extreme near-field enhancement makes the slit region, which

#102270 - $15.00 USD Received 1 Oct 2008; revised 19 Nov 2008; accepted 20 Nov 2008; published 25 Nov 2008

also happens to be the focal region of the probing laser beam, to be the prime source of the signal. Away from the slit, the field amplitude quickly diminishes. In addition, the Gaussian laser beam samples broader and broader regions away from the slit, where amplitudes with different phases may cancel each other, again helping us to probe only the extreme near-field.

We have demonstrated, using terahertz Fourier-transform near-field imaging with ~λ/100 resolution, the occurrence of a large field enhancement at the fundamental shape resonance. Remarkably, the field enhancement increases with increasing a_y/a_x ratio and therefore with decreasing slit width. To achieve the highest field enhancement at a given frequency then, one needs to design the slit length to be half the wavelength and the slit width to be as narrow as possible. This intriguing result can be understood if we realize that at resonance, the same amount of energy has to funnel through the slit no matter how narrow it is. The extremely large aspect ratio rectangular slits with large field enhancement would find immediate application in physics, engineering and biology where large and controllable terahertz field enhancement is much desired. In principle, using these slits, the largest field enhancement one can achieve would be of the order of λ/δ where δ is the skin depth. This amount of field enhancement could make it possible to perform nonlinear experiments starting from common laboratory terahertz sources.

Acknowledgments

Research support from the Korean government (Korean Science and Engineering Foundation, Ministry of Science and Technology, Ministry of Commerce, Industry, and Energy, and Ministry of Education, Seoul R&BD program) and the EU TERANOVA Program (RCN-71835) are acknowledged.

#102270 - $15.00 USD Received 1 Oct 2008; revised 19 Nov 2008; accepted 20 Nov 2008; published 25 Nov 2008